Nonlinear Control of a High-Purity Distillation Column Using a Traveling-Wave Model

Lalitha S. Balasubramhanya and Francis J. Doyle III
School of Chemical Engineering, Purdue University, West Lafayette, IN 47907

The trade-off between model accuracy and computation tractability for model-based control applications is well known. While nonlinear models are needed to capture the detailed behavior of many chemical processes, the resultant structures may not lead to straightforward control implementation. The current work advocates the use of low-order nonlinear models based on wave propagation that are mathematically concise and capture the essential nonlinear behavior of a process. In this work, differential geometry is invoked to achieve input–output linearization of a high-purity distillation column based on a traveling-wave model. A Kalman filter is used to recursively update the parameter values. Comparison with a linear controller based on a two-time constant model shows that the nonlinear controller outperforms the linear controller in tight control of both the overhead and the bottoms composition.

Introduction

Process models are an integral component of most computer-integrated process operations (Bassett et al., 1994). Control schemes, optimization, process scheduling, fault diagnosis, all rely heavily on the process description. Independent of the specific design technique employed, the majority of the process controllers are based on some form of model describing the dynamic behavior of the process, be it just the process gain and the settling time, or systems of partial differential equations (Morari and Zafiriou, 1989).

Traditionally, linear models are used as approximations to the real plant, as they are simple to understand, easy to obtain and, furthermore, linear control theory is a well-developed discipline. The drawbacks associated with the linear models, however, are that they are often valid only in a small neighborhood of the nominal operating point and cannot capture the rich nonlinear behavior of many processes. The use of a linear control scheme can limit the achievable performance if the process is highly nonlinear (Bequette, 1991). Given the nonlinearities that characterize chemical processes, the design of nonlinear controllers is well motivated.

The last decade has seen a significant increase in the number of control-system techniques that are based on nonlinear systems concepts (Allgöwer and Doyle III, 1997). Progress in nonlinear control theory, combined with computer hardware advances now allow advanced, nonlinear control strategies to be successfully implemented on chemical processes (Allgöwer and Doyle III, 1997). Nonlinear model development is an extremely important part of nonlinear model-based strategy (Bequette, 1991). There is a growing need to develop modeling strategies that can capture the nonlinear behavior of processes for application in nonlinear control.

Models developed from first principles are a descriptive source of information for any process. However, they are invariably complex, coupled, nonlinear partial differential equations. Methods such as finite differences and orthogonal collocation can be used to simplify these equations, but they lead to a large number of ordinary differential equations (Cho and Joseph, 1984). Hankel reduction, balanced realization, and other techniques can be used for reducing the order of the equations, but the resulting equations do not retain their physical significance (Marquardt, 1985). Similarly, data-driven models, based on only the input–output information, do not always capture the physically significant parameters. Understanding the physical significance of parameters and variables is often helpful in developing a good control strategy. An example is the linear two time-constant model for distillation columns developed by Skogestad and Morari (1988b) where the two time constants that capture the dynamic behavior of the column are motivated by the internal and external flows in the column. There is a need for low-order nonlinear models that can capture the essential nonlinearity of the system

Correspondence concerning this article should be addressed to F. J. Doyle III.

while retaining mathematical simplicity as well as physical significance.

Systems with distributed parameters often exhibit dynamic phenomena that resembles traveling waves. Conservation of mass, energy and momentum often results in traveling waves that can be represented by wavefronts, wave pulses, and wave trains (Marquardt, 1990). In chemical engineering, the propagation of waves has been studied extensively in connection with reaction engineering, combustion technology, and separation processes. Examples include temperature and composition profiles in high-purity distillation columns (Luyben, 1972), temperature profiles in fixed-bed reactors (Puszyński and Hlavacek, 1984), and composition profiles in adsorption columns.

The objective of this article is to utilize the traveling-wave phenomenon exhibited by a high-purity distillation column in developing low-order models to capture its nonlinear behavior and develop model-based control strategies to control the process.

Nonlinear Control of Distillation Columns

Tight control of high-purity distillation columns has been a subject of research for many years (for review, see, for example, Luyben, 1992; Skogestad, 1992). Controller designs based upon linearized and lumped models work reasonably well for columns of low to moderate purity. Increasing demands of high product quality, minimal waste generation, and low energy consumption have led to an increased demand for tighter control of columns. The performance of linear model-based control systems degrades in applications to high-purity columns, particularly for dual-composition control (Lévine and Rouchon, 1991).

One of the first researchers to use traveling waves in control applications was Luyben (1972). The profile position of the temperature front in a distillation column was used as the controlled variable in rejecting feed disturbances. Nandakumar and Andres (1981) use the wave model to calculate the minimum reflux conditions. Based on the profile position, Gilles and Retzbach (1983) developed a simple dynamic model for an extractive distillation column with a vapor side stream. They linearized the model obtained and utilized it for regulatory control.

Marquardt (1986, 1988, 1990) studied the behavior of the traveling waves in great detail, most notably in applications to high-purity distillation columns. Using various approximations for the vapor liquid equilibrium, he was able to derive theoretical expressions for the composition profiles in the column. The parameters in the profiles were obtained using the method of weighted residuals. Temperatures in the column were measured and the compositions were inferred using a Kalman filter. The model thus obtained was linearized and used in linear control.

Hwang extended the well-developed theories from fixed-bed sorption to countercurrent separation processes and discussed the formation of self-sharpening waves in high-purity distillation columns (Hwang, 1991). He attributed the traveling of composition waves to imbalances in the convective transport between the two phases. The model developed by Hwang is discussed in some detail in the next section.

Han and Park (1993) used the concise model developed by Hwang in a generic model control algorithm (GMC). The profile positions in the rectifying and the stripping sections were taken to be the states of the system. The error weighting factor of the observer was defined as a nonlinear empirical function of the distance from the profile position. Composition measurements were taken at every tray to correct the estimated value of the states.

In the recent years, it has been shown that nonlinear state feedback controllers can be used effectively to achieve good control of nonlinear systems. Groebel et al. (1994) used asymptotically exact input–output linearization of a detailed, tray-by-tray model to control an industrial distillation column. Regular input–output linearization did not give linear responses or disturbance decoupling. However, they demonstrated that an additional compensator could be introduced to linearize the system. Lévine and Rouchon (1991) used nonlinear aggregate models to control distillation columns. They reduced the detailed model to compartments based on the time scale of the response to the changes in the manipulated variables and the disturbances. Differential geometry was then used to linearize the model and control the plant. A similar approach was also taken by Castro and Alvarez (1990), where they used a bilinear estimation technique for a low-order aggregated distillation column model. McLellan et al. (1990) demonstrated that distillation columns satisfy the "disturbance decoupling" conditions, that is, the disturbances do not directly affect the outputs and can be decoupled from the outputs. Alsop and Edgar (1990) used approximate linearization in conjunction with a low-order nonlinear multiple input/multiple output (MIMO) model of a distillation column for nonlinear control of a rigorous distillation column.

Nonlinear variable transformation has been another approach taken by many to combat the nonlinearity of the process. Joseph and Brosilow (1978) and Ryskamp (1982) used the logarithms of the outputs to implicitly decouple the controllers. Skogestad and Morari (1988a,b) demonstrated that scaling based on logarithms eliminated nonlinearity at high frequency and the subsequent controller operated effectively over a wide range of operating conditions. Mountziaris and Georgiou (1988) derived various nonlinear transformations and evaluated them based on steady-state control design tools such as the relative gain array.

In the next few sections our approach to the problem is outlined, where the model based on the traveling-wave phenomenon is utilized in nonlinear feedback-control strategy to obtain tight control of a high-purity distillation column.

Nonlinear Wave Theory

A traveling wave is defined as a structure moving with a constant propagation velocity and constant shape along a spatial coordinate. The dynamic behavior of a distillation column can be characterized by the movement of the composition or the temperature profiles up or down the column in response to the feed disturbances or changes in manipulated variables (Hwang, 1991; Marquardt, 1990).

The mass balance for the entire rectifying section of a distillation column can be written as the following partial differential equation:

$$\frac{\partial x}{\partial \tau} + r\frac{\partial y}{\partial \tau} - \frac{L}{F}\frac{\partial x}{\partial \sigma} + \frac{V}{F}\frac{\partial y}{\partial \sigma} = 0. \qquad (1)$$

Here x is the mole fraction of the more volatile component in the liquid stream; y is the mole fraction in the vapor stream; L and V are the liquid and vapor flow rates in the section; F is the feed flow rate; σ is the normalized tray position; τ is the normalized time; and r is the ratio of the vapor to liquid holdup. The velocity along constant x is given by

$$v = \left(\frac{\partial \sigma}{\partial \tau}\right)_{x,y} = \frac{V}{F}\frac{\frac{dy}{dx} - \frac{L}{V}}{1 + r\frac{dy}{dx}}, \tag{2}$$

where dy/dx is the slope of the equilibrium. Equation 2 represents the normalized wave velocity. It is apparent that each point on the composition profile moves with a different velocity. If v_x tends to decrease with σ, then the wave tends to sharpen; if v_x tends to increase with σ, then the wave spreads. The former is called a self-sharpening wave and the latter a nonsharpening wave. At the point where dy/dx is equal to the slope of the operating line L/V, the velocity is zero (stagnation point). A self-sharpening wave eventually becomes a discontinuity at this point. The subsequent movement of the wave can be characterized by its shock-wave velocity, v_Δ, which is obtained from a global material balance across the wave:

$$v_\Delta = \left(\frac{\partial \sigma}{\partial \tau}\right)\Delta = \frac{V}{F}\frac{\frac{\Delta y}{\Delta x} - \frac{L}{V}}{1 + r\frac{\Delta y}{\Delta x}}. \tag{3}$$

The concentration profile moves with this shock velocity when a disturbance perturbs the system. As the wave travels to the end of the column, nonequilibrium forces dominate, forcing the wave to stop, thereby establishing a new steady state that depends on the new L/V.

Equations 2 and 3 are relevant for the rectifying section of the column. Similar equations can also be written for the stripping section. The shock-wave velocity is given by

$$v_\Delta = \left(\frac{\partial \sigma}{\partial \tau}\right)\Delta = \frac{\bar{L}}{F}\frac{\frac{\bar{V}}{\bar{L}}\frac{\Delta y}{\Delta x} - 1}{1 + r\frac{\Delta y}{\Delta x}}, \tag{4}$$

where $\bar{L}$ and $\bar{V}$ are the liquid and the vapor flow rates in the stripping section. A simple mass balance around the feed tray links the two sections.

The two differential Eqs. 3 and 4 describe the motion of the stagnation points (s_{rec} and s_{strip}) or the fronts of the waves. These distinct fronts are related to the regions of intense mass transfer. The shape of the wave is principally determined by the vapor–liquid–equilibrium (VLE). Marquardt (1986) analytically derived expressions for the shape of the wave for different VLE relations. In this work, a wave profile is employed that is similar to the analytical solution for a second-order VLE relationship. The expression is shown in Eq. 5 where γ_r, $\gamma_{r\min}$, and $y_{r\max}$ determine the shape (y_l and y_e are the vapor concentrations leaving and entering the rectifying section). More complicated expressions are obtained for the shape profile when complex expressions are used for the VLE. This expression was selected over others, as it captures the shape of the profiles observed for the case study considered. The parameters have a simple physical interpretation as well. $y_{r\min}$ and $y_{r\max}$ fix the boundary of the profile while γ_r determines the steepness of the profile:

$$y_l = y_{r\min} + \frac{y_{r\max} - y_{r\min}}{1 + \exp(-\gamma_r(1 - s_{rec}))}$$

$$y_e = y_{r\min} + \frac{y_{r\max} - y_{r\min}}{1 + \exp(\gamma_r s_{rec})}. \tag{5}$$

Similar equations can also be derived for the stripping section.

For the sake of completeness, the assumptions made for the derivation of the reduced model are provided: (1) ideal equilibrium stages; (2) constant relative volatility for the VLE relationships; (3) total condenser and reboiler; (4) constant molar overflow; (5) constant molar holdup of all the plates with the same value; (6) constant liquid holdup; and (7) negligible vapor holdup of the reboiler and the condenser. Furthermore, the energy balances are neglected.

Marquardt and Amrhein (1994) derive an additional term in describing the velocity of the wave that is attributed to the change in shape of the profile. However, it is also stated in their article that this term is generally small compared to the contribution of the net flow (derived in Eqs. 3 and 4) and hence can be neglected. Moreover, in this approach, the change in shape of the profiles is handled using a parameter estimator, as is shown in the following sections.

The constant model structure approach can be compared to the approaches taken by other researchers who have proposed low-order *empirical* models. Skogestad and Morari (1988b) use the logarithms of the overhead and the bottom compositions, and fit the resulting linear model to a two time-constant equation. Wong and Seborg (1992) assume a nonlinear structure in which the gain and the time constants are empirically dependent on the output. Chien and Ogunnaike (1992) assumed a similar structure, but in their model the gain and the time constant depend empirically on the input. A notable distinction of the structure used in this work over preceding structures is the fact that this approach is based on a fundamental process description.

Parameter Estimation

In the model described in the previous section, there are three parameters to be determined in each section of the column. In this approach, the parameters $y_{r\max}$, $y_{r\min}$, $y_{s\max}$, and $y_{s\min}$ are fixed. The mismatch between the plant and the model is lumped in the shape parameters γ_r and γ_s, and they are varied to ensure that the model tracks the plant closely. To do so, the parameters are estimated using a filter and the mismatch is represented as noise, which is filtered. A similar approach for estimation of parameters is presented in (Gelb, 1974). Using this approach the nonlinear wave model can be represented as

$$\dot{\gamma}_r = \omega_1$$

$$\dot{\gamma}_s = \omega_2$$

$$\dot{s}_{\text{rec}} = \frac{1}{1+r\left(\frac{\Delta y}{\Delta x}\right)_r}\left[\frac{V_{\text{nom}}}{F}\left(\frac{\Delta y}{\Delta x}\right)_r - \frac{L_{\text{nom}}}{F} - \frac{u_1}{F} + \left(\frac{\Delta y}{\Delta x}\right)_r \frac{u_2}{F}\right] + \omega_3$$

$$\dot{s}_{\text{strip}} = \frac{1}{1+r\left(\frac{\Delta y}{\Delta x}\right)_s}\left[\frac{\bar{V}_{\text{nom}}}{F}\left(\frac{\Delta y}{\Delta x}\right)_s - \frac{\bar{L}_{\text{nom}}}{F} - \frac{u_1}{F} + \left(\frac{\Delta y}{\Delta x}\right)_s \frac{u_2}{F}\right] + \omega_4$$

$$\left(\frac{\Delta y}{\Delta x}\right)_r = \frac{y_{r\min} + \dfrac{y_{r\max} - y_{r\min}}{1+\exp[-\gamma_r(1-s_{\text{rec}})]} - y_1}{y_{r\min} + \dfrac{y_{r\max} - y_{r\min}}{1+\exp[-\gamma_r(1-s_{\text{rec}})]} - \dfrac{y_{r\max} + y_{r\min}\exp(\gamma_r s_{\text{rec}})}{2 + y_{r\max} + (2+y_{r\min})\exp(\gamma_r s_{\text{rec}})}}$$

$$\left(\frac{\Delta y}{\Delta x}\right)_s = \frac{\dfrac{y_{s\max} - y_{s\min}}{1+\exp(\gamma_s s_{\text{strip}})} - \dfrac{y_{s\max} - y_{s\min}}{1+\exp[-\gamma_s(1-s_{\text{strip}})]}}{y_{s\min} + \dfrac{y_{s\max} - y_{s\min}}{1+\exp(\gamma_s s_{\text{strip}})} - x_2}$$

$$y_1 = \frac{\alpha x_2}{1-(\alpha-1)x_2}$$

$$0 = Vy_1 + (L+F)x_2 - Fz_f - Lx_1 - Vy_2$$

$$y = (y_d + \nu_1 \; y_b + \nu_2)^T. \tag{6}$$

Here, L_{nom} and V_{nom} are the liquid and vapor flow rates at the nominal operating point; y_d and y_b are the overhead and the bottoms compositions (calculated using the equation for the wave shape, Eq. 5); and u_1 and u_2 are the liquid and vapor flow rates, respectively, in deviation variables. The mass balance around the feed tray is an algebraic constraint that links the two differential equations. The feed coming in is assumed to be saturated liquid. x_1 is the mole fraction of the lighter component in the liquid stream leaving the rectifying section, y_1 is the vapor mole fraction of the component entering the rectifying section, x_2 is the mole fraction of the component in the liquid stream entering the stripping section, and y_2 is the mole fraction of the component in the vapor stream leaving the stripping section. y_1 and x_2 satisfy the equilibrium relationship, where α is the relative volatility. ω_1, ω_2, ω_3, ω_4, ν_1, and ν_2 are independent white-noise processes.

The algebraic constraint is satisfied numerically, resulting in four nonlinear, coupled differential equations that can be represented as

$$\dot{x} = \left[\dot{\gamma}_r \dot{\gamma}_s \dot{s}_{\text{rec}} \dot{s}_{\text{strip}}\right]^T = f(x) + g_1(x)u_1 + g_2(x)u_2 + [\omega_1 \omega_2 \omega_3 \omega_4]^T. \tag{7}$$

The states of the reduced model, x, have to be estimated using the output measurements from the detailed column model. Here, the Kalman filter is invoked to estimate the states. Let $A = [\partial f(x)]/\partial x$, $C = [\partial h(x)]/\partial x$, Q, the covariance of the process noise, and R, the covariance of the measurement noise. Then the matrix differential equation for the covariance of the states is given by

$$\frac{dP}{dt} = AP + PA^T + Q - PC^T R^{-1} CP$$

$$K = PC^T R^{-1}, \tag{8}$$

where K is the Kalman gain matrix (Gelb, 1974); A and C are obtained at the nominal operating point and used in the preceding calculation; the steady-state values of P, and hence K, can be calculated off-line to yield a suboptimal filter. The estimates of the states in Eq. 7 can be obtained using

$$\dot{\hat{x}} = f(\hat{x}) + K(y - \hat{y}) + g_1(\hat{x})u_1 + g_2(\hat{x})u_2$$

$$\hat{y} = h(\hat{x}), \tag{9}$$

where y is the observation from the plant, $\hat{y}$ is the estimated value, and $K(y - \hat{y})$ is the filtered error that is fed back to update the states.

The Kalman filter for this system gives very good estimates of the stagnation points, s_{rec} and s_{strip}, as well as the parameters, γ_r and γ_s. The case study in the sixth section shows that this approach ensures that the reduced model tracks the detailed column accurately.

Control Design

For the distillation column, the manipulated variables considered here are the liquid and vapor flow rates, and the controlled outputs are the overhead and bottoms mole fraction of the lighter component. The L/V configuration is chosen here, as this is the one most commonly used in industry (Skogestad and Morari, 1988a). By a suitable transformation of variables, other configurations such as D/V and D/B can also be considered. The control strategy adopted is input–output linearization that has been used in many process-control applications (Kravaris and Chung, 1987). The key idea involves a nonlinear coordinate transformation, based on differential geometry, that converts a nonlinear system into a linear system relating the output y to a new input v in the transformed coordinates. Algebraic equations link

the new input v and u. Using this method, a multivariable system cannot only be linearized, it can often be decoupled as well. The resultant decoupled, linear systems can be controlled using linear controllers (Kravaris and Soroush, 1990).

Two aspects of this problem make the use of differential geometry challenging: (1) the system is modeled using differential algebraic equations as opposed to simply differential equations; and (2) the incorporation of a Kalman filter, which gives an estimate of the stagnation points as well as the parameters, adds a new disturbance to the system.

Kalman filter in control design

The presence of a Kalman filter introduces an additional term, $K(y-\hat{y})$, in the model as is shown in Eq. 9. Since $\hat{y}$ is a function of $\hat{x}$, it can be included in the $f(\hat{x})$ term. However, Ky acts as an additional disturbance affecting the system. The outputs have a relative degree of $(1,1)^T$ with respect to this disturbance.

$$f_{\text{est}}(\hat{x}) = f(\hat{x}) - K\hat{y}. \tag{10}$$

Instead of f, f_{est} is used in the calculation of the Lie derivatives, that is, $L_{f_{\text{est}}}h$, $L_g L_{f_{\text{est}}}h$. This modification accounts for the presence of the filter in the control design.

This modification is referred to as asymptotically exact linearization by Groebel et al. (1994). They use this technique to control a distillation column using temperature measurements. The error between the estimated and measured temperature is filtered and used in input/output linearization. The advantage of this method is that the states of the model, which are required for feedback linearization, are completely known since the filter is used to estimate them.

Differential Algebraic Equations. McClamroch (1990), Fliess et al. (1994), and Kumar and Daoutidis (1995) are some of the researchers who have used differential geometry to linearize a system of differential-algebraic equations. The presence of the algebraic constraints complicates the control strategy, particularly if the system has an index greater than one.

In particular, Kumar and Daoutidis (1994) have looked at chemical engineering problems that are modeled by differential algebraic equations. Consider a system that is represented by the following equations:

$$\begin{aligned} \dot{x} &= f(x) + g(x)u + b(x)z \\ 0 &= k(x) + l(x)z, \end{aligned} \tag{11}$$

where z is an algebraic variable. If the system has index 1, then $l(x)$ is nonsingular and

$$z = -l(x)^{-1}k(x). \tag{12}$$

The expression obtained for z from Eq. 12 is substituted in Eq. 11 to obtain a set of differential equations. (The more complicated case of linearization when the index is greater than one is dealt with in Kumar and Daoutidis (1995).)

To apply the method just described, the wave model (Eq. 9) has to be rewritten. Define:

$$\begin{aligned} m(\hat{x}) &\doteq K\hat{y} \\ d &\doteq Ky \\ \delta y &\doteq d - m(\hat{x}) = K(y-\hat{y}), \end{aligned} \tag{13}$$

where $\hat{y}$ is the estimated value of the outputs; y is the array of the measurements of the outputs from the detailed model; $\Delta y/\Delta x$, evaluated as per Eq. 6, is a complicated function of the states. Then the equations can be written as

$$\begin{aligned} \dot{\hat{x}} = &\begin{bmatrix} -m_1 \\ -m_2 \\ \dfrac{V_{\text{nom}}}{F}\dfrac{\left(\dfrac{\Delta y}{\Delta x}\right)_r}{1+r\left(\dfrac{\Delta y}{\Delta x}\right)_r} - m_3 \\ \dfrac{1}{1+r\left(\dfrac{\Delta y}{\Delta x}\right)_s}\left[\dfrac{V_{\text{nom}}}{F}\left(\dfrac{\Delta y}{\Delta x}\right)_s - 1\right] - m_4 \end{bmatrix} \\ &+ \begin{bmatrix} 0 \\ 0 \\ \dfrac{-1}{F\left[1+r\left(\dfrac{\Delta y}{\Delta x}\right)_r\right]} \\ \dfrac{-1}{F\left[1+r\left(\dfrac{\Delta y}{\Delta x}\right)_s\right]} \end{bmatrix} L_{\text{nom}} + \begin{bmatrix} 0 \\ 0 \\ \dfrac{-1}{F\left[1+r\left(\dfrac{\Delta y}{\Delta x}\right)_r\right]} \\ \dfrac{-1}{F\left[1+r\left(\dfrac{\Delta y}{\Delta x}\right)_s\right]} \end{bmatrix} u_1 \\ &+ \begin{bmatrix} 0 \\ 0 \\ \dfrac{1}{F\left[1+r\left(\dfrac{\Delta y}{\Delta x}\right)_r\right]}\left(\dfrac{\Delta y}{\Delta x}\right)_r \\ \dfrac{1}{F\left[1+r\left(\dfrac{\Delta y}{\Delta x}\right)_s\right]}\left(\dfrac{\Delta y}{\Delta x}\right)_s \end{bmatrix} u_2 + d \\ &= f_{\text{est}}(\hat{x}) + p(\hat{x})L_{\text{nom}} + g_1(\hat{x})u_1 + g_2(\hat{x})u_2 + d \\ 0 &= Vy_1 + (L+F)x_2 - Fz_f - Lx_1 - Vy_2 \\ \hat{y} &= h(\hat{x}) = [y_d(\hat{x})\ y_b(\hat{x})]^T. \end{aligned} \tag{14}$$

For this case the index of the system is one which implies that the constraints can be rewritten as

$$\begin{aligned} 0 &= (-Fz_f + V_{\text{nom}}y_1 - V_{\text{nom}}y_2 + Fx_2) + L_{\text{nom}}(x_2 - x_1) \\ &\quad + (x_2 - x_1)u_1 + (y_1 - y_2)u_2 \\ L_{\text{nom}} &= \frac{V_{\text{nom}}y_1 + Fx_2 - Fx_f - V_{\text{nom}}y_2}{x_1 - x_2} - u_1 + \frac{y_1 - y_2}{x_1 - x_2}u_2 \\ L_{\text{nom}} &= k(\hat{x}) + l_1(\hat{x})u_1 + l_2(\hat{x})u_2. \end{aligned} \tag{15}$$

We can rewrite the model equations as

$$\dot{\hat{x}} = \bar{f}(\hat{x}) + \bar{g}_1(\hat{x})u_1 + \bar{g}_2(\hat{x})u_2 + d$$
$$\hat{y} = [h_1(\hat{x}) \quad h_2(\hat{x})]^T, \tag{16}$$

where

$$\bar{f}(\hat{x}) = f_{est}(\hat{x}) + p(\hat{x})k(\hat{x})$$
$$\bar{g}_1(\hat{x}) = g_1(\hat{x}) + p(\hat{x})l_1(\hat{x})$$
$$\bar{g}_2(\hat{x}) = g_2(\hat{x}) + p(\hat{x})l_2(\hat{x}). \tag{17}$$

This is a simple extension of the approach taken by Kumar and Daoutidis (1995) to include the input terms in the constraint. The model can now be treated as nonlinear differential equations that can be linearized using the input–output linearization scheme.

An alternative approach to the problem is to satisfy the constraint numerically and treat the model as nonlinear differential equations. This results in numerical simplifications, as $\bar{f}$, $\bar{g}_1$, and so on, are not evaluated. A similar approach is used by Groebel et al. (1994). The vector relative degree is calculated to be $(1, 1)^T$, the sum of which is less than the number of states, 4. This implies that two of the transformed states can be linearized using new inputs, while the other two will form the internal states of the system. The nonlinear coordinate transformation Ψ is chosen to be

$$z_1 = h_1(\hat{x})$$
$$z_2 = h_2(\hat{x})$$
$$z_3 = \hat{x}(1)$$
$$z_4 = \hat{x}(2). \tag{18}$$

This ensures the transformation is diffeomorphic, as the Jacobian of Ψ is nonsingular. In the new coordinates the equations can now be written as

$$\dot{z}_1 = L_{f_{est}}h_1 + L_{g_1}h_1u_1 + L_{g_2}h_1u_2 + d_1$$
$$\dot{z}_2 = L_{f_{est}}h_2 + L_{g_1}h_2u_1 + L_{g_2}h_2u_2 + d_2$$
$$\dot{z}_3 = \dot{\hat{x}}(1) = -m_1 + d_1 = \delta y_1(\hat{x}, d)$$
$$\dot{z}_4 = \dot{\hat{x}}(2) = -m_2 + d_2 = \delta y_2(\hat{x}, d) \tag{19}$$

New inputs, v_1 and v_2, are introduced and related to the old inputs, u_1 and u_2, via the following equations in the transformed coordinates:

$$L_{f_{est}}h_1 + L_{g_1}h_1u_1 + L_{g_2}h_1u_2 + d_1 = \dot{z}_1 = \frac{v_1}{\alpha_1} - \frac{\alpha_0}{\alpha_1}z_1$$
$$L_{f_{est}}h_2 + L_{g_1}h_2u_1 + L_{g_2}h_2u_2 + d_2 = \dot{z}_2 = \frac{v_2}{\beta_1} - \frac{\beta_0}{\beta_1}z_2. \tag{20}$$

Rearrangement of the righthand side of the preceding equations results in two decoupled, first-order linear systems.

$$\alpha_1\frac{dz_1}{dt} + \alpha_0 z_1 = v_1$$
$$\beta_1\frac{dz_2}{dt} + \beta_0 z_2 = v_2. \tag{21}$$

$z_1 = y_1(\hat{x})$ and $z_2 = y_2(\hat{x})$ are linear with respect to the new inputs v_1 and v_2. The presence of the filter ensures that $y_1(\hat{x})$ and $y_2(\hat{x})$ track the output measurements from the plant, y_1 and y_2, closely. Hence the plant can be linearized and decoupled as well.

As is seen from the preceding equations, the stability and the response characteristics of z_1 and z_2 can be manipulated using the tuning parameters. However, apart from them, the internal states (z_3 and z_4), that is, the zero dynamics need to be stable as well for the system to be stable. The stability of the internal states can be analyzed from the behavior of $\dot{z}_3 = \dot{\hat{x}}(1)$ and $\dot{z}_4 = \dot{\hat{x}}(2)$, which depends on the stability of the filter (Eq. 9). For a localized stability analysis the linearized version of Eq. 9 is considered:

$$\dot{\hat{x}} = A\hat{x} + Bu + K(y - C\hat{x})$$
$$\dot{\hat{x}} = (A - KC)\hat{x} + Bu + Ky$$
$$\hat{y} = C\hat{x}. \tag{22}$$

Here

$$B = \frac{\partial[g_1(x) \quad g_2(x)]}{\partial x},$$
$$u = [u_1 \quad u_2]^T,$$
$$A = \frac{\partial f(x)}{\partial x}, \quad \text{and} \quad C = \frac{\partial h(x)}{\partial x}.$$

The preceding system is stable for bounded inputs (u and y) only if all the eigenvalues of the matrix $A - KC$ are in the left half plane. For this case, three of the eigenvalues are in the left half plane and one is very close to zero, that is, almost on the $j\omega$ axis (though still in the left half plane). Extensive simulations over a large range of operating points indicate that the system is indeed stable and the parameters are bounded. Some of the simulations are presented in the section discussing the case study. The eigenvalue close to zero corresponds to the stagnation position in the rectifying section, s_{rec}. This can be rectified by obtaining temperature measurements along the length of the column to map out the profile and hence increase the robustness of the observer. However, in this work, the simplest measurement set is assumed (endpoint only), while a more elaborate inferential scheme requiring profile measurement is left for future work. Thus, the nonlinear model can be decomposed into two decoupled, first-order linear systems, and the internal states of the system are stable as well. Two linear internal model controllers (IMCs) can be used to close the outer loops. α_0, α_1, β_0, and β_1 are tuned to meet the closed-loop requirements.

Changes in the feed flow rate and the feed composition constitute measured disturbances that affect the system. Calculations indicate that the system has a higher relative degree with respect to these disturbances than the manipulated variables, therefore the nominal design will achieve perfect disturbance rejection (for no model mismatch). In a way this

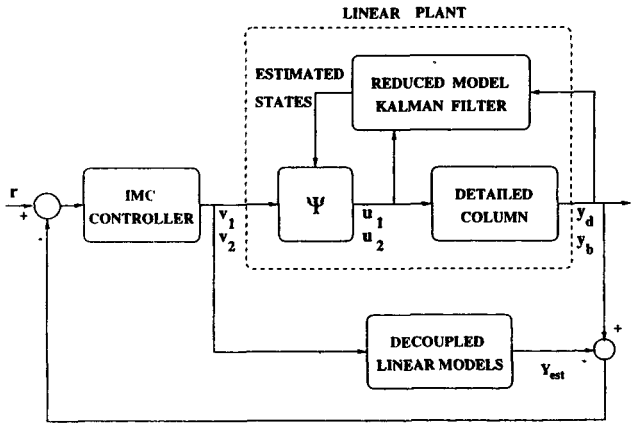

Figure 1. Diagram of the controller.

design incorporates feedforward control, since the nonlinear model takes into consideration the values of the feed flow rate and the feed composition.

A diagram of the complete setup including the controller and the estimator is shown in Figure 1.

Case Study

The case study under consideration is a 20-tray distillation column separating an equimolar mixture of benzene and toluene (see Table 1). The model used is an industrially relevant case study in the dynamic simulation solver SPEEDUP. Detailed energy balances, temperature and composition-dependent VLE, and the hydrodynamics of the flow in the column are modeled in this case study. This detailed SPEEDUP model is a reasonably complex realistic model to capture the nonlinear behavior of a distillation column. The relative volatility of the mixture is approximately equal to 2.0. Additional results for controlling the column are presented in Balasubramhanya and Doyle III (1995). The column is highly nonlinear with strong dependence of the gains and the lags on the magnitude and the direction of the disturbances. Another indication of the nonlinearity of this system is the variation of its relative gain array (RGA), which is a scalar control-relevant trend, with respect to the operating level. In this case, the operating regime is determined by varying the composition of the feed entering the column. A linear model will predict a single RGA value, while a nonlinear model gives rise to a locus of RGA values. Figure 2 shows how the RGA varies with the operating point.

Table 1. Nominal Operating Conditions in Detailed Column and Reduced Model

	Detailed	Reduced
Reflux (kmol/h)	130.069	102.371
Vapor (kmol/h)	175.67	151.939
Feed (kmol/h)	100	100
Feed mole fraction	0.5	0.5
Top mole fraction	0.985	0.985
Bottom mole fraction	23.34*e*-3	23.34*e*-3
No. of ODEs	89	2
y_{rmin}	—	0.62
y_{rmax}	—	1
y_{smin}	—	0.0005
y_{smax}	—	0.75

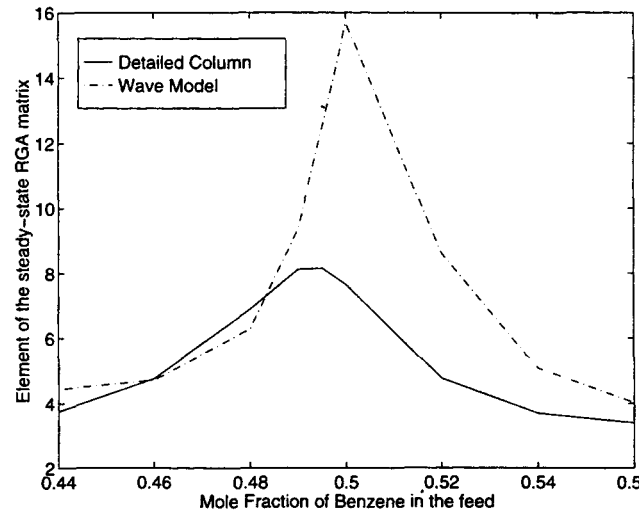

Figure 2. Relative gain array as a function of the operating point (Kalman filter not used to update the parameters).

The change in the RGA can be used as a control-relevant parameter to validate a reduced model. The reduced model under consideration is the nonlinear wave model discussed previously (see Table 1). The parameters y_{rmin}, y_{rmax}, y_{smin}, and y_{smax} are fixed empirically using the compositions entering and leaving the rectifying and stripping sections of the detailed column. Constant values of γ_r and γ_s are used instead of estimating them at each operating point. As γ_r and γ_s are fixed and not estimated each time, the feed composition information is not used in calculating the RGA. As shown in Figure 2, the reduced model is able to capture the change in RGA. A linear model would have a constant RGA evaluated at the nominal operating point. If the plant were to operate at a point away from the nominal operating point, model mismatch would be introduced in a linear control configuration, as the linear model cannot capture the variation in the RGA. Other researchers have plotted RGA as function of frequency yielding linear analysis results (e.g., Skogestad and Morari, 1988b; Amrhein et al., 1993). In the present work, the emphasis is more on the *nonlinear* variation of RGA with a change in the operating point.

Singular-value decomposition (SVD) of the steady-state gain matrix for the detailed column and the reduced model can provide important information regarding the input directions that give rise to the maximum and the minimum gains (Amrhein et al., 1993). The SVD of the gain matrix for the detailed column at the nominal operating point is given by

$$\begin{bmatrix} 4.58345E-3 & -4.50812E-3 \\ 8.66812E-3 & -9.80880E-3 \end{bmatrix} = \begin{bmatrix} 4.40303E-1 & -8.97849E-1 \\ 8.97849E-1 & 4.40303E-1 \end{bmatrix} \times \begin{bmatrix} 1.45780E-2 & 0 \\ 0 & 4.03430E-4 \end{bmatrix} \times \begin{bmatrix} 6.72300E-1 & -7.40279E-1 \\ -7.40279E-1 & -6.73200E-1 \end{bmatrix}. \quad (23)$$

Similar decomposition for the gain matrix of the reduced model at the nominal operating point gives

$$\begin{bmatrix} 1.13604E-2 & -1.10322E-2 \\ 7.90035E-3 & -8.22294E-3 \end{bmatrix} = \begin{bmatrix} 8.11551E-1 & -5.84282E-1 \\ 5.84282E-1 & 8.11551E-1 \end{bmatrix} \times \begin{bmatrix} 1.95115E-2 & 0 \\ 0 & 3.20727E-4 \end{bmatrix} \times \begin{bmatrix} 7.09100E-01 & -7.05108E-1 \\ -7.05108E-1 & -7.09100E-1 \end{bmatrix}. \quad (24)$$

Maximum and minimum singular values are the maximum and minimum gains of the plants (Skogestad and Morari, 1988b), as the inputs are varied. It is essential that a model be able to capture this information as well as the input directions associated with them. The singular values for the reduced model and the detailed model are extremely close. The unitary matrices for the detailed column corresponding to the gains are captured closely by the reduced model, particularly the righthand unitary matrix. The importance of capturing not just the singular values but the directions accurately is stressed by Amrhein and Marquardt (1993).

Skogestad and Morari (1988b) also illustrated how a distillation column can be represented by a linear model that accounts for the two inherent time constants in the column corresponding to the internal and external flows. The two time constants for the detailed column are 2.465 and 0.529 h (obtained as per the equations in Skogestad and Morari (1988b)). The reduced model when linearized about the nominal operating point, is a second-order model with the time constants 2.492 and 0.220 h. The dominant time constants for both the models are very close and the internal time constants are of the same order of magnitude.

The reduced model is also validated by conducting open-loop simulations. The liquid flow rate to the column is increased by 10%. Figure 3 shows that the reduced model does indeed capture the behavior of the detailed model (the plot for bottoms composition of the reduced model overlays the plot for the detailed model). A Kalman filter is used to update the values of the shape parameters and address the plant model mismatch. The variation in the parameters for this case is shown in Figure 4.

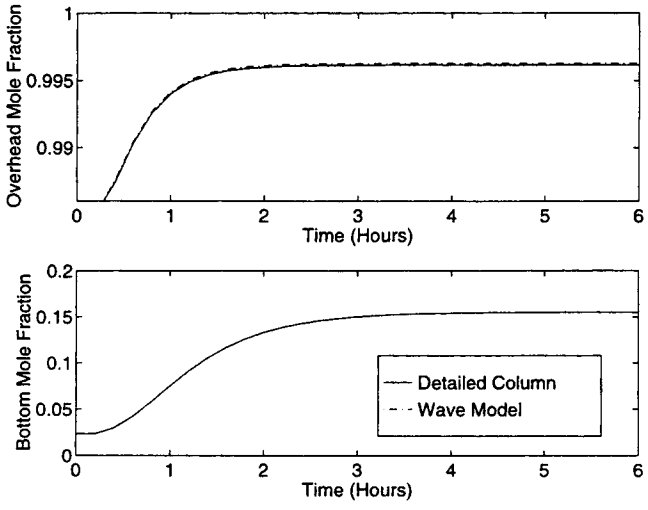

Figure 3. Open-loop responses of the detailed and the reduced models for a step change of 10 kmol/h in the liquid flow rate (Kalman filter used to update the parameters).

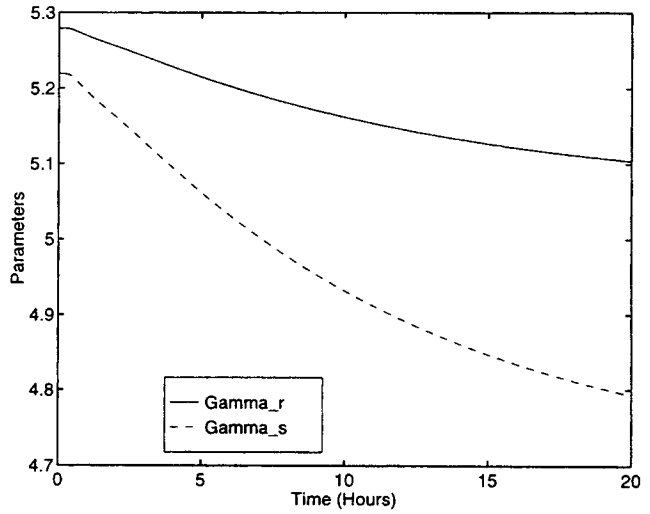

Figure 4. Variation in the parameters for an open-loop step change of 10 kmol/h change in the liquid flow rate.

Another issue of importance is whether the estimator is sensitive to uncertainties in the initial values for the parameters. To study this, a 25% error in the initial value of γ_r and a 25% error in γ_s were introduced and the response of the reduced model was plotted. As can be observed from Figure 5, the reduced model tracks the detailed column model within a very short span of time. The change in the states of the observer (parameters as well as the stagnation positions) for this case is shown in Figure 6.

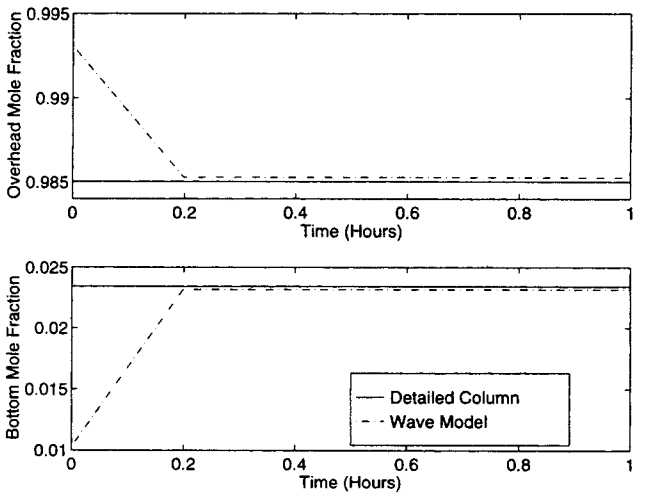

Figure 5. Open-loop response of the reduced model with incorrect initial parameter values (+25% error in γ_r and γ_s).

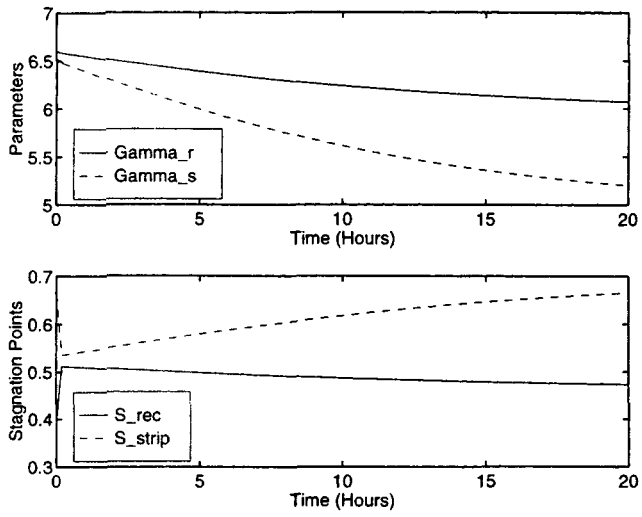

Figure 6. Change in the states of the observer, γ_r, γ_s, s_{rec}, and s_{strip}, for incorrect initial parameter values (open loop; +25% error in γ_r and γ_s).

As described earlier, the reduced model has a vector-relative degree, and hence can be decoupled and linearized. An open-loop simulation of the linear system relating y and v is carried out by changing the input v_1 while keeping v_2 constant. The results are shown in Figure 7 where the ideal response (no model mismatch—dashed line) is compared to the true column response (solid line) and the wave model (dotted-dashed line). The response of the wave model completely overlays the ideal response indicating that it is completely decoupled and linearized. The true column shows very small deviations, and it can be assumed that the true column is decoupled and linearized as well.

Closed-loop simulations were carried out to verify the controller performance. The performance of the nonlinear controller was compared to linear IMC controllers. The Jacobian about the nominal operating point provides information about

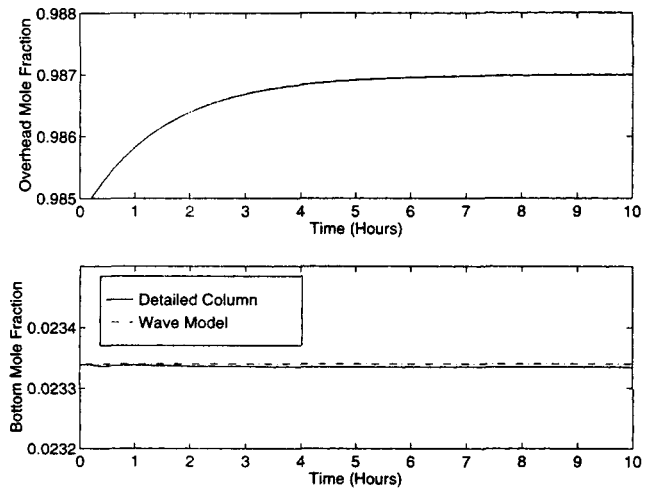

Figure 7. Open-loop step change of +0.02 in the transformed input v_1 keeping v_2 constant shows linear, decoupled response.

the gains of the column. A simple linear model can be obtained using the Jacobian and a single time constant as shown:

$$G_1(s) = \frac{1}{2s+1}\begin{bmatrix} 4.58345E-3 & -4.50812E-3 \\ 8.66812E-3 & -9.80880E-3 \end{bmatrix}. \quad (25)$$

A linear IMC controller would include the inverse of the model and a filter to tune the response of the system:

$$C_1(s) = \frac{1}{\lambda s+1} G_1^{-1}(s). \quad (26)$$

As was mentioned earlier, Skogestad and Morari (1988a) demonstrated that a two time-constant model captures the high-frequency behavior of the column better than a single time-constant model. A two time-constant model with the time constants of 2.465 and 0.529 h was also used to develop an IMC controller:

$$G_2(s) = \begin{bmatrix} \dfrac{4.58345E-3}{2.465s+1} & \dfrac{-4.58345E-3}{2.465s+1} + \dfrac{7.733E-5}{0.529s+1} \\ \dfrac{8.66812E-3}{2.465s+2} & \dfrac{-8.66812E-3}{2.465s+1} + \dfrac{-1.14068E-3}{0.529s+1} \end{bmatrix}$$

$$C_2(s) = \frac{1}{\lambda s+1} G_2^{-1}(s). \quad (27)$$

For both the linear controllers $\lambda = 1.5$ h. For the nonlinear controller, $\alpha_0 = \beta_0 = 1$ and $\alpha_1 = \beta_1 = 1.5$. These settings ensure that both the linear and nonlinear controllers have a closed-loop time constant of 1.5 h in the overhead and the bottoms loop.

A setpoint change in the bottom composition is used to compare all the three controllers. Figure 8 shows that while

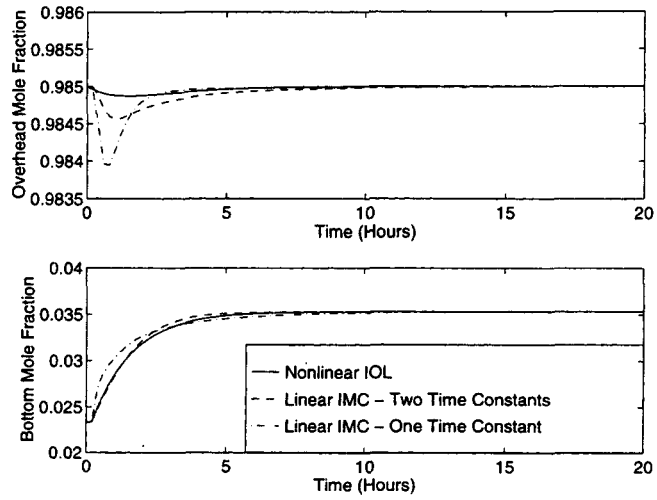

Figure 8. Closed-loop step change of +0.012 in the mole fraction of benzene in the bottoms.

Comparison between the performance of the nonlinear controller, the linear controller based on a single time constant model, and the linear controller based on the two time-constant model is provided.

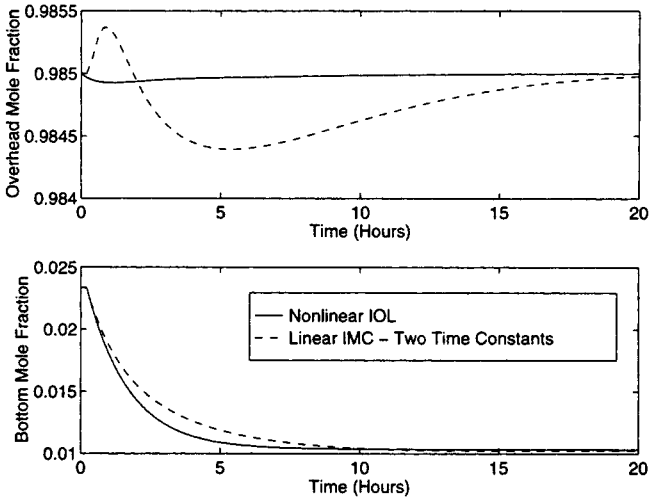

Figure 9. Closed-loop response to a step change in the setpoint of the bottoms composition, $r = (0, -0.013)^T$.

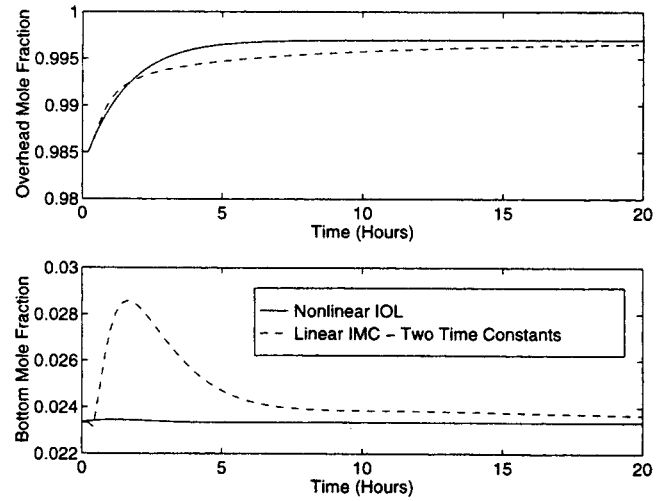

Figure 11. Closed-loop response to a step change in the setpoint of the overhead composition, $r = (0.0120, 0)^T$.

the controller based on the two time-constant model has a smaller settling time for both the loops than the one based on the one time-constant model, the nonlinear controller outperforms both the linear controllers. "Nonlinear IOL" refers to the response of the detailed column in conjunction with the IOL controller while "Linear IMC" refers to the response of the detailed column in conjunction with a linear controller. Henceforth only comparison with the two time-constant linear controller will be provided.

A setpoint change in the bottom composition in the other direction is considered. From Figure 9 it is evident that although the performance of both the controllers is comparable in the bottom loop, the nonlinear controller outperforms the linear controller in controlling the overhead composition. Figure 10 shows the variation in the parameters for the setpoint change.

Next, changes in the overhead composition were considered. An increase in the overhead composition is shown in Figure 11. As the figure indicates, the nonlinear controller outperforms the linear controller in dual control of the compositions. The input move for this setpoint change is shown in Figure 12, which shows that the moves dictated by the nonlinear controller are not drastic or difficult to implement.

Disturbance rejection is of critical importance for high-purity column operation. A comparison between the linear and the nonlinear controllers is shown in Figure 13. A feedforward/feedback IMC controller designed for disturbance rejection and setpoint control is used as the linear controller. The nonlinear model incorporates information about the feed flow and the feed composition in its formulation, leading to implicit feedforward compensation. The disturbance is a change in the feed flow rate from 100 kmol/h to 120 kmol/h.

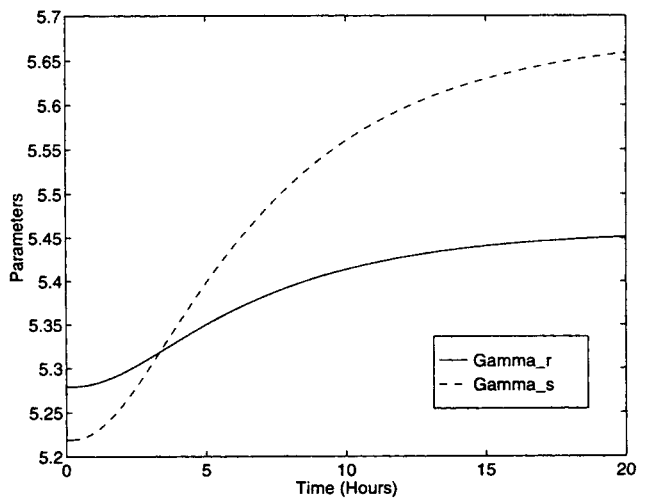

Figure 10. Change in the parameters for a closed-loop setpoint change in the bottoms composition, $r = (0, -0.013)^T$.

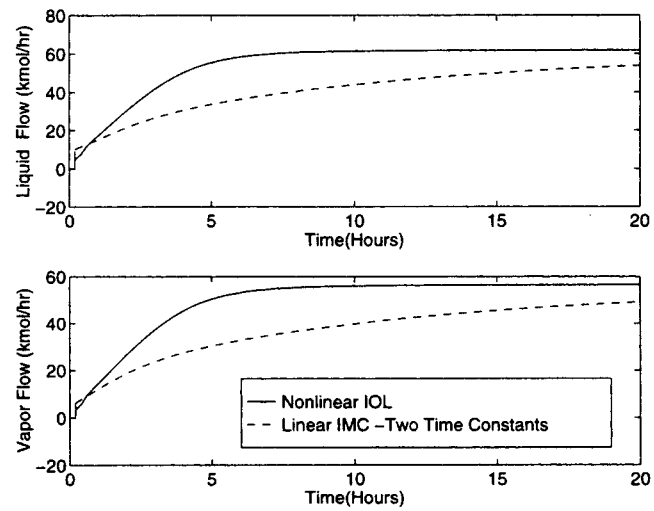

Figure 12. Inputs move for a closed-loop step change in the setpoint of the overhead composition, $r = (0.0120, 0)^T$.

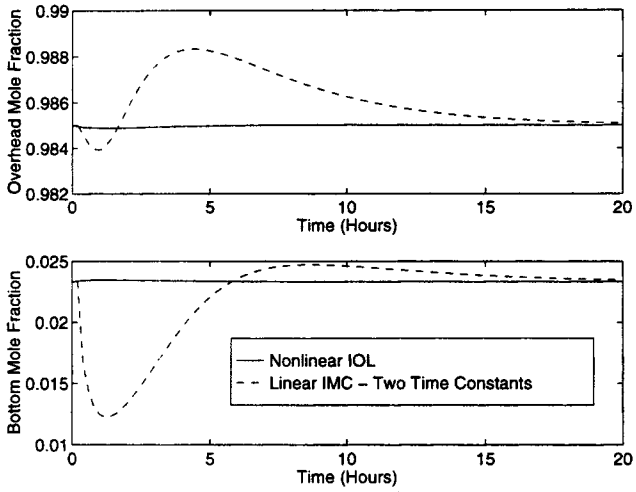

Figure 13. Closed-loop response for a 20% step change in the feed flow rate (disturbance rejection).

As is evident from Figure 13, the nonlinear control achieves a tighter regulation of both the overhead and bottom compositions compared to the linear controller.

Conclusions

The theory of traveling waves provides a simple, elegant, and nonlinear model to capture the dynamic behavior of a high-purity distillation column. Assumptions regarding a constant structure for the shape of the profiles provides further simplification of the problem. The shape parameters of the profile are updated on-line using a Kalman filter, for which the gains can be calculated off-line. The nonlinear model is able to capture certain inherent behavior of a distillation column, such as variation in the RGA with operating points, the two time constants, the singular gains, and input directions. Furthermore, the reduced model lends itself to input–output linearization via state feedback. A comparison is provided between a linear controller based on the two time-constant model and the nonlinear controller, in which it is observed that the nonlinear controller outperforms the linear controller in dual composition control. Significantly improved disturbance rejection is also obtained using the nonlinear controller.

Thus, the dynamic behavior of a process can be used to develop nonlinear models for use in nonlinear control strategies, resulting in tight control. Application of traveling waves in other unit operations such as pulp-digesters and reactive distillation columns are areas of future interest to the authors.

Acknowledgments

One of the authors (F.J.D.) acknowledges the support of NSF through a Young Investigator Award (CTS-9257059). The other author (L.S.B.) acknowledges additional funding from a Purdue David Gross Grant and the Purdue Computer Integrated Process Operations Consortium (CIPAC).

Literature Cited

Allgöwer, F., and F. J. Doyle III, "Nonlinear Process Control—Which Way to the Promised Land?," *Proc. CPC V*, in press (1997).

Alsop, A. W., and T. F. Edgar, "Nonlinear Control of a High-Purity Distillation Column by the Use of Partially Linearized Control Variables," *Comput. Chem. Eng.*, **14**, 665 (1990).

Amrhein, M., F. Allgöwer, and W. Marquardt, "Validation and Analysis of Linear Distillation Models for Controller Design," *Proc. European Control Conf.*, Groningen, The Netherlands (1993).

Balasubramhanya, L. S., and F. Doyle III, "Low Order Modeling for Nonlinear Process Control," *Proc. American Control Conf.*, Seattle, WA, p. 2682 (1995).

Bassett, M. H., P. Dave, F. J. Doyle, G. Kudva, J. F. Pekny, G. V. Reklaitis, S. Subrahmanyam, M. Zentner, and D. Miller, "Perspectives on Model Based Integration of Process Operations," *Proc. Process Systems Engineering Conf.*, Kyongju, Korea (1994).

Bequette, B. W., "Nonlinear Control of Chemical Processes: A Review," *Ind. Eng. Chem. Res.*, **30**(7), 1391 (1991).

Castro, R., and J. Alvarez, "Nonlinear Disturbance Decoupling Control of a Binary Distillation Column," *Automatica*, **26**, 567 (1990).

Chien, I. L., and B. A. Ogunnaike, "Modeling and Control of High-Purity Distillation Columns," AIChE Meeting, Miami (1992).

Cho, Y. S., and B. Joseph, "Reduced-Order Models for Separation Columns, Part III," *Comput. Chem. Eng.*, **8**, 81 (1984).

Fliess, M., J. Levine, P. Martin, and P. Rouchon, "Nonlinear Control and Lie-Backlund Transformations: Towards a New Differential Geometric Standpoint," *Proc. IEEE Conf. on Decision Control*, IEEE, Piscataway, NJ, p. 339 (1994).

Gelb, A., ed., *Applied Optimal Estimation*, M.I.T. Press, Cambridge, MA (1974).

Gilles, E. D., and B. Retzbach, "Reduced Models and Control of Distillation Columns with Sharp Temperature Profiles," *IEEE Trans. Automat. Contr.*, **AC-28**, 628 (1983).

Groebel, M., F. Allgöwer, M. Storz, and E. D. Gilles, "Nonlinear Control of High Purity Distillation Columns," AIChE Meeting, San Francisco (1994).

Han, M., and S. Park, "Control of High-Purity Distillation Column Using a Nonlinear Wave Theory," *AIChE J.*, **39**(5), 787 (1993).

Hwang, Y. L., "Nonlinear Wave Theory for Dynamics of Binary Distillation Columns," *AIChE J.*, **37**(5), 705 (1991).

Joseph, B., and C. Brosilow, "Inferential Control of Processes," *AIChE J.*, **24**(3), 485 (1978).

Kravaris, C., and C. B. Chung, "Nonlinear State Feedback Synthesis by Global Input/Output Linearization," *AIChE J.*, **33**, 592 (1987).

Kravaris, C., and M. Soroush, "Synthesis of Multivariable Nonlinear Controllers by Input/Output Linearization," *AIChE J.*, **36**(2), 249 (1990).

Kumar, A., and P. Daoutidis, "Feedback Control of Nonlinear Differential Algebraic-Equation Systems," *AIChE J.*, **41**(3), 619 (1995).

Lévine, J., and P. Rouchon, "Quality Control of Binary Distillation Columns Based on Nonlinear Aggregated Models," *Automatica*, **27**(3), 463 (1991).

Luyben, W. L., "Profile Position Control of Distillation Columns with Sharp Temperature Profiles," *AIChE J.*, **18**, 238 (1972).

Luyben, W. L., ed., *Practical Distillation Control*, Van Nostrand Reinhold, New York (1992).

Marquardt, W., "Model Reduction Techniques for Separation Columns," *Proc. Int. Conf. Industrial Process Modelling and Control* (1985).

Marquardt, W., "Nonlinear Model Reduction for Binary Distillation," *DYCORD*, published by IFAC, Bournemouth, UK, p. 123 (1986).

Marquardt, W., "Nichtlineare Wellenausbreitung—Ein Weg zu Reduzierten dynamischen Modellen von Stofftrennprozessen," PhD Thesis, Univ. of Stuttgart, Stuttgart, Germany (1988).

Marquardt, W., "Traveling Waves in Chemical Processes," *Int. Chem. Eng.*, **30**(4), 585 (1990).

Marquardt, W., and M. Amrhein, "Development of a Linear Distillation Model from Design Data for Process Control," *Comput. Chem. Eng.*, **18**, S349 (1994).

McClamroch, N. H., "On Control Systems Described by a Class of Nonlinear Differential-Algebraic Equations: State Realizations and Local Control," *Proc. Amer. Control Conf.*, p. 1701 (1990).

McLellan, P. J., T. J. Harris, and D. W. Bacon, "Disturbance Decou-

pling of Staged Processes," *Proc. American Control Conf.*, p. 2729 (1990).
Morari, M., and E. Zafiriou, *Robust Process Control*, Prentice Hall, Englewood Cliffs, NJ (1989).
Mountziaris, T. J., and A. Georgiou, "Design of Robust Noninteracting Controllers for High-Purity Binary Distillation Columns," *Ind. Eng. Chem. Res.*, **27**(8), 1450 (1988).
Nandakumar, K., and R. P. Andres, "Minimum Reflux Conditions: I. Theory: II. Numerical Solution," *AIChE J.*, **27**(3), 450 (1981).
Puszyński, J., and V. Hlavacek, "Experimental Study of Ignition and Extinction Waves and Oscillatory Behavior of a Tubular Nonadiabatic Fixed Bed Reactor for the Oxidation of Carbon Monoxide," *Chem. Eng. Sci.*, **39**(4), 681 (1984).
Ryskamp, C., "Explicit vs. Implicit Decoupling in Distillation Control," *Chemical Process Control*, Vol. II, D. Seborg and T. Edgar, eds., United Engineering Trustees, New York (1982).
Skogestad, S., "Dynamics and Control of Distillation Columns," (survey paper) *DYCORD*, p. 1 (1992).
Skogestad, S., and M. Morari, "LV-Control of a High-Purity Distillation Column," *Chem. Eng. Sci.*, **43**(1), 33 (1988a).
Skogestad, S., and M. Morari, "Understanding the Dynamic Behavior of Distillation Columns," *Ind. Eng. Chem. Res.*, **27**, 624 (1988b).
Wong, S. K. P., and D. E. Seborg, "Low Order, Nonlinear, Dynamic Models for Distillation Columns," AIChE Meeting, Miami (1992).

Manuscript received Apr. 8, 1996, and revision received Sept. 18, 1996.